

Destructive Instabilities in Hollow Intense Relativistic Electron Beams

C. A. Kapetanakos, D. A. Hammer, and C. D. Striffler*
Naval Research Laboratory, Washington, D. C. 20375

and

R. C. Davidson†
*Naval Research Laboratory, Washington, D. C. 20375, and University of Maryland,
 College Park, Maryland 20742*
 (Received 12 December 1972)

It is found that a 400-keV, 10–40-kA, 50-nsec duration hollow relativistic electron beam suffers from a severe instability when injected into neutral gas along a magnetic field. The dependence of beam distortion on beam thickness, magnetic field strength, beam current, and proximity of the surrounding conducting walls is experimentally studied. The experimental observations are consistent with the diocotron instability occurring during the first several nanoseconds of the beam pulse.

Magnetically focused, hollow cylindrical, relativistic electron beams are utilized for the production of high-power microwaves¹ and are of interest for plasma heating² because they allow the propagation of higher current density than solid beams. In this Letter we report that under a wide range of experimental conditions hollow relativistic electron beams suffer from an instability that destroys the beam. Although the observed destruction of the beam is not necessarily the result of the evolution of a single instability, there is strong evidence that the diocotron instability is operative during the first several nanoseconds of the beam pulse and is responsible for the characteristic features of the experimental observations. It is interesting to note that the present experimental results are similar to those obtained³ with beams having more than 3 orders of magnitude lower voltage and 6 orders of magnitude lower current.

A schematic of the experiment is shown in Fig. 1. The 50-nsec-duration electron beam is produced by a 7- Ω coaxial, water dielectric, Blumlein pulse-forming line. The 400-keV electron pulse is emitted by a 5-cm outside-diameter annular graphite cathode separated by a gap of ~ 0.5 cm from the 0.0025-cm-thick titanium anode. We used three cathodes with annular thicknesses of 0.6, 0.3, and ≤ 0.1 cm (wedge shaped). Typically, the beam current is 40 kA, but some data have been taken with beam current as low as 10 kA. Upon passing through the anode foil, the beam enters an 8.8-cm-diam Lucite drift tube lined with copper mesh and containing air between 0.1 and 0.2 Torr pressure. The cathode-anode

gap and the drift region are immersed in a uniform applied solenoidal magnetic field. The beam shape after drifting is inferred from the damage done to a Lucite plate placed in the beam path. For lower current experiments, typically 15 kA, the Lucite is replaced by radiation sensitive paper (EG & G radiachromic paper RACM 301).

It is observed that at the anode, and for short distances thereafter (~ 6 cm), the electron beam is cylindrically symmetric. However, it becomes progressively more distorted as it travels longer distances. Figures 2(a)–2(d) show the damage patterns resulting from four shots with the Lucite located at distances at 10, 35, 45, and 52 cm, respectively, from the anode using the 0.3-cm-thick annular cathode at 4.0 kG. Similar results are obtained with the other two cathodes. Specifically, it is found that the 0.6-cm-thick annular

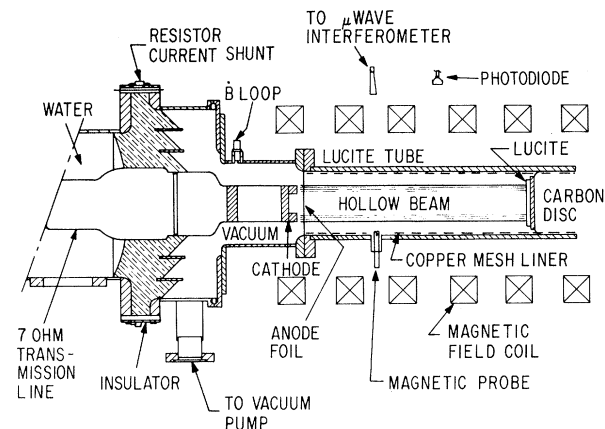


FIG. 1. Schematic of the experiment.

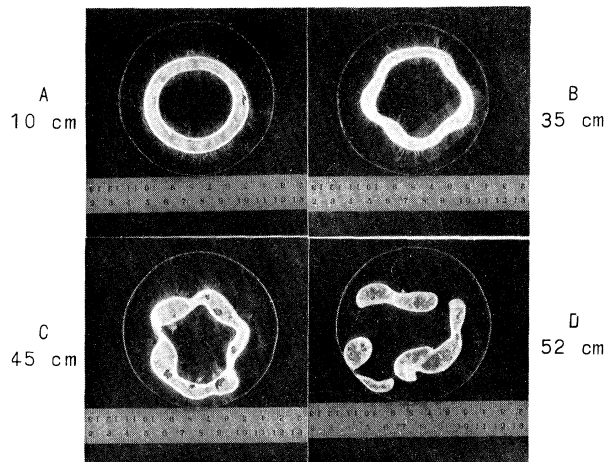


FIG. 2. Lucite damage patterns at various distances from the anode using the 0.3-cm-thick annular cathode. Beam parameters are 40-kA and 400-kV peak voltage. Drift tube pressure is $\sim 200 \mu\text{m}$ of air.

beam is typically unstable to $l=3$ or $l=4$ modes. The 0.3-cm-thick beam is unstable to $l=5$ or 6, and the beam from the wedge-shaped cathode typically shows higher l values dominating the damage pattern. The distortion is significantly reduced by bringing the conducting boundary near to the outer edge of the beam. Furthermore, it is observed that the beam distortion increases for higher beam current and/or lower magnetic fields.

By passing the beam through several (typically five) 6×10^{-4} -cm-thick sheets of aluminized Mylar placed 2.7 cm apart, it is found that both azimuthal and axial wave numbers are present in the distorted beam. For a beam current density of 5 kA/cm², beam voltage of 400 keV, and applied magnetic field of approximately 2 kG, the axial wavelength λ_z is about 27 cm. At 4-kG magnetic field, λ_z is considerably longer than 27 cm and rather difficult to measure with any reasonable accuracy.

Using magnetic probes 2 mm in diameter and having a frequency response better than $4 \times 10^8 \text{ sec}^{-1}$, it has been determined that the avalanche breakdown time of the ~ 0.2 Torr air is between 5 and 8 nsec. From the decay of magnetic probe traces it is estimated that the resulting plasma resistivity is approximately $10^{-3} \Omega \text{ cm}$, corresponding to an electron plasma temperature of about 10 eV.

Some data have also been taken at neutral gas pressures above 0.2 Torr and at a few milli Torr. Data at high pressure, i.e., ~ 0.5 Torr, indicate

that the distortion in the beam is less than that observed in the pressure range 0.1–0.2 Torr. At low pressure, as expected, the beam propagates poorly and most of the beam is lost after traveling a few centimeters in the drift tube. Even at axial positions very near to the anode (1–2 cm), the Lucite damage patterns show a considerable expansion of the electron beam when the pressure is in the milli Torr range.

The observed avalanche breakdown time of 5–8 nsec at 0.2 Torr indicates that the beam is susceptible to nonresistive instabilities during the first few nanoseconds of the beam pulse. For the remainder of the pulse, it is reasonable to expect that beam-plasma streaming instabilities (electrostatic or electromagnetic) may be operative, and that these instabilities are responsible for our observations since most of the beam duration is available to them. However, as discussed by Benford,⁴ if nonresistive instabilities do occur, they may affect the evolution of modes growing after breakdown. Electromagnetic modes are expected to be unstable and have sufficiently fast growth rates for the parameters of our experiment.⁴ However, the experimental observations are not consistent with their expected “signature,” since the theoretical growth rates do not depend on mode number l , and are affected by an outer conducting wall only if it is within c/ω_p of the beam surface. Electrostatic two-stream instabilities can be eliminated for our beam and boundary parameters because of finite radial geometry effects.⁵

The diocotron instability,⁶ appropriately extended to include relativistic beam dynamics and a partially neutralizing ion background,⁷ explains the key features of the experimental observations. The theory assumes that an infinitely long, cylindrically symmetric annular electron beam of inner radius b and outer radius c propagates inside a conducting cylinder (radius d) and along an applied magnetic field $B_0 \hat{z}$ (see inset, Fig. 3). In equilibrium, the beam density N is assumed to be uniform within the annulus and all electrons have the same relativistic axial velocity V_B . The beam charge is partially neutralized by an infinitely massive ion background in the annulus having density fN , where $0 \leq f \leq 1$. We use a cold-fluid description of the electron beam in the low-density approximation ($\omega_p^2 \ll \omega_c^2$). In equilibrium, the beam is characterized by an azimuthal rotational velocity $V_D(r)$, given by ($b \leq r \leq c$)

$$V_D(r) = \frac{1}{2}(\omega_p^2/\omega_c)(1-f-\beta_B^2)r(1-b^2/r^2), \quad (1)$$

where $\omega_p \equiv (4\pi Ne^2/m\gamma)^{1/2}$, $\omega_c \equiv eB_0/m\gamma c$, $\beta_B = V_B/c$, and $\gamma \equiv (1 - V_D^2/c^2 - V_B^2/c^2)^{-1/2}$. Equation (1) is obtained from equilibrium force balance in the radial direction including the effects of the radial self-electric and azimuthal self-magnetic fields.

Since the damage plates in Fig. 2 are indicative

of steady ($\partial/\partial t = 0$) spatial growth in the z direction, the linear electrostatic stability of the system is examined by assuming the perturbed quantities to have dependence of the form $\tilde{f}(r) \exp(il\theta + ik_z z)$, where k_z is the (complex) axial wave number. Assuming $\omega_p^2 \ll \omega_c^2$ and $\omega_p^2 \ll l^2 V_B^2/c^2$, the dispersion relation for $l \geq 1$ is found to be

$$\frac{(k_z V_B)^2}{\omega_D^2} + \frac{k_z V_B}{\omega_D} \left[\frac{c^{2l} - b^{2l}}{d^{2l}} + l \frac{(1 - f\gamma_B^2)}{\gamma_B^2} \frac{c^2 - b^2}{c^2} \right] - \left[\frac{(d^{2l} - c^{2l})(c^{2l} - b^{2l})}{d^{2l} c^{2l}} - l \frac{(1 - f\gamma_B^2)}{\gamma_B^2} \frac{c^2 - b^2}{c^2} \frac{(d^{2l} - b^{2l})}{d^{2l}} \right] = 0, \tag{2}$$

where $\gamma_B^{-2} = 1 - \beta_B^2$, $\omega_D \equiv \frac{1}{2}\omega_p^2/\omega_c$ is the diocotron frequency, and we have assumed $V_D^2 \ll V_B^2$. This equation is similar to that derived by Levy⁶ with the replacement $k_z V_B \rightarrow -\omega$. The factor $(1 - f\gamma_B^2)/\gamma_B^2$ is 1 in his analysis, since $f = 0$ and $\gamma_B = 1$. For $b \neq 0$ and $c \neq d$, we obtain from Eq. (2) that $f \geq \gamma_B^{-2} = 1 - \beta_B^2$ is a sufficient condition for stability ($\text{Im}k_z = 0$) for all values of l . Figure 3 displays the unstable regions for the $l = 2-6$ modes (the $l = 1$ mode is stable). In contrast to the results obtained for $f = 0$ and $\gamma_B = 1$,⁶ Fig. 3 indicates that the lower modes ($l = 2$ and 3) are *not* always unstable ($\text{Im}k_z < 0$) when instability does exist at higher l values. For thinner beams, the unstable regions for each mode number shift towards lower values of f and γ_B , and these regions begin to overlap.

The most important point of agreement between the experimental observations and the diocotron mode is the azimuthal mode dependence with beam thickness. As indicated in Fig. 3, a specific l value is predicted to be unstable for a particular geometry, f , and γ_B . According to Eq. (2), for a given f and γ_B , when the beam thickness decreases, higher l values become unstable. Moreover, enhanced overlapping of unstable regions occurs for thinner beams, i.e., two or more l values become unstable. Another important point of agreement is the stabilizing effect of bringing the conducting boundary closer to the beam boundary [Eq. (2) predicts that the unstable regions in f - γ_B space vanish as d approaches c]. We also note that Eq. (2) predicts that the axial wavelength $[2\pi/\text{Re}(k_z)]$ and growth length $[1/\text{Im}(k_z)]$ are directly proportional to B_0 and inversely proportional to beam density (or current) for any given l value and geometric configuration, in agreement with observation.

Parameters appropriate to the first few nanoseconds of the beam (it takes 4-5 nsec for the

beam front to traverse the drift tube and, at any given axial position in the tube, ≈ 5 nsec for $f > \gamma_B^{-2}$ to be achieved) for the experiments shown in Fig. 2 are $\omega_p \approx 3.5 \times 10^{10} \text{ sec}^{-1}$, $\omega_c \approx 5.5 \times 10^{10} \text{ sec}^{-1}$, and $V_B \approx 2 \times 10^{10} \text{ cm/sec}$. For the $l = 5$ mode this yields a minimum growth length of 6 cm, consistent with observations. In the experiments in which the wavelength is measurable, appropriate early-time parameters are $\omega_p \approx 2 \times 10^{10} \text{ sec}^{-1}$, $\omega_c \approx 3 \times 10^{10} \text{ sec}^{-1}$, and $V_B \approx 2 \times 10^{10} \text{ cm/sec}$. For the $l = 3$ mode, these parameters give a minimum axial wavelength of 12 cm (obtained by setting $f = 0$ and $\gamma_B = 1$). However, since $f \neq 0$ and $\gamma_B \neq 1$, the actual wavelength is longer. Note that the required inequalities $\omega_p^2 \ll \omega_c^2$ and $\omega_p^2 \ll l^2 V_B^2/c^2$ are marginally satisfied for $B_0 \approx 2 \text{ kG}$. The inclusion of the effects of shear in V_B (due to the beam's self-potential well)⁸ along with the azimuthal shear (i.e., diocotron), ap-

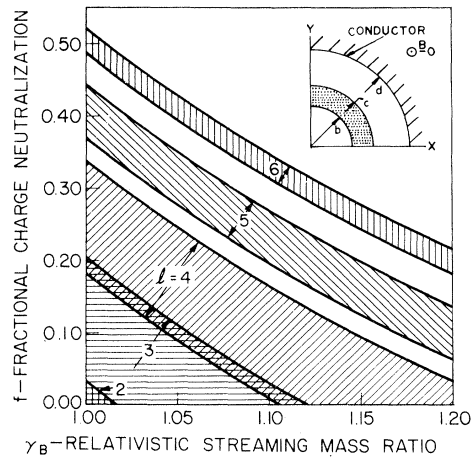


FIG. 3. Stability-instability regions in f - γ_B space as a function of mode number l . Shaded regions correspond to instability. Geometry: $b = 1.6$, $c = 2.8$, and $d = 5.0$ cm. Inset: geometry of theoretical model.

pears to decrease the growth length insignificantly except for short axial wavelengths, which are not observed.

In summary, the characteristic features of the diocotron instability correlated well with the experimental observations. It appears that the beam distortion is produced at early time, i.e., before $f > \gamma_B^{-2}$, and when breakdown of the background gas occurs shortly thereafter, it occurs along the distorted path of the beam, and the beam follows that path for the remaining 40 nsec.

We have benefitted greatly from our discussions with M. Lampe and R. N. Sudan, and we would like to thank R. Covington for his expert technical assistance.

*National Research Council—Naval Research Labora-

tory Resident Research Associate.

†Research supported in part by the U. S. Office of Naval Research and in part by the National Science Foundation.

¹M. Friedman and M. Herndon, Phys. Rev. Lett. 28, 210 (1972), and 29, 55 (1972).

²C. A. Kapetanakos, D. A. Hammer, I. Haber, and W. M. Black, Bull. Amer. Phys. Soc. 17, 1032 (1972).

³R. L. Kyhl and H. F. Webster, IRE Trans. Electron Devices 3, 172 (1956).

⁴G. Benford, Phys. Rev. Lett. 28, 1242 (1972), and to be published.

⁵L. S. Bogdankevich and A. A. Rukhadze, Usp. Fiz. Nauk 103, 609 (1971) [Sov. Phys. Usp. 14, 163 (1971)].

⁶R. H. Levy, Phys. Fluids 8, 1288 (1965).

⁷C. D. Striffler, D. A. Hammer, C. A. Kapetanakos, and R. C. Davidson, Bull. Amer. Phys. Soc. 17, 1032 (1972).

⁸J. A. Rome and R. J. Briggs, Phys. Fluids 15, 796 (1972).

Nonlinear Interaction of Electromagnetic Waves in a Plasma Density Gradient*

Allan N. Kaufman and Bruce I. Cohen

Department of Physics and Lawrence Berkeley Laboratory, University of California, Berkeley, California 94720

(Received 10 May 1973)

Two intense electromagnetic waves interact strongly where the local plasma frequency equals their difference frequency, resulting in an irreversible transfer of action from the higher-frequency wave to the lower-frequency wave. The amount of transfer depends only on the intensities and the density scale length. Successive transfers among a set of waves may produce efficient plasma heating.

Interest in the nonlinear interaction between coherent electromagnetic waves arises from the possibility of exciting longitudinal plasma modes in an underdense ($\omega_p \ll \omega$) plasma by resonance with the difference frequency of two lasers,¹ thereby heating the plasma upon damping of the longitudinal modes. This process has been studied by Rosenbluth and Liu² for an inhomogeneous plasma, but neglecting the reaction of the longitudinal mode on the transverse waves; and by Cohen, Kaufman, and Watson,³ including the reaction and allowing for a cascade, but for a homogeneous plasma.

The present paper treats the transfer of energy between two transverse waves (of frequencies ω_0, ω_1 with $\omega_0 > \omega_1$) in a plasma density gradient. The mechanism of the transfer is the resonant excitation of an electron longitudinal mode at the beat frequency $\Omega \equiv \omega_0 - \omega_1$ and beat wave number $K \equiv k_0 + k_1$ (for the optimum case of opposed lasers, which we consider for definiteness). The excitation occurs over a zone of thickness $h \sim (\nu/\omega_p)L$ about the surface where $\omega_p = \Omega$; L is the

density scale length, and ν the longitudinal damping rate.

We stress two important conclusions⁴: (1) The dominant effect of the process is the transfer of action ΔJ from the higher-frequency (ω_0) wave to the lower-frequency (ω_1) wave, transverse action being conserved. Accordingly, the energy loss $\omega_0 \Delta J$ of the ω_0 wave is partitioned, with $\omega_1 \Delta J$ going to the ω_1 wave, and $\Omega \Delta J$ being irreversibly deposited in the plasma. The maximum heating efficiency is thus Ω/ω_0 . (That this ratio is low for an underdense plasma led us in Ref. 3 to suggest cascading; we return to this below.) (2) The total amount of action transfer depends on the input power and on the density scale, but is *independent* of the damping rate⁵ ν (as long as WKB conditions are satisfied: $h \gg k^{-1}$). There is thus no need to be concerned with the damping mechanism, be it collisional, Landau, or nonlinear.

Our formulation of the interaction is in terms of the local longitudinal dielectric function, and thus is quite model independent. For simplicity

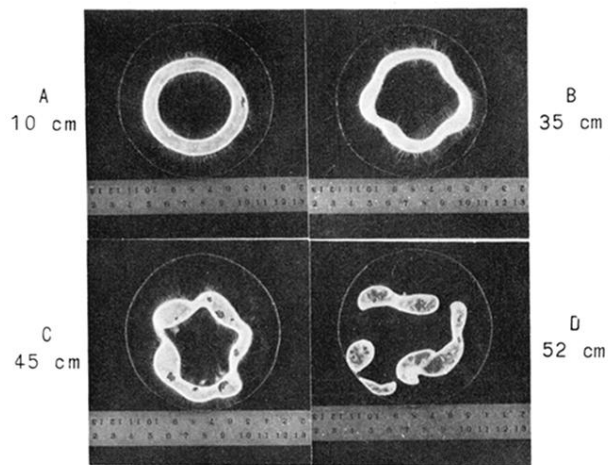


FIG. 2. Lucite damage patterns at various distances from the anode using the 0.3-cm-thick annular cathode. Beam parameters are 40-kA and 400-kV peak voltage. Drift tube pressure is $\sim 200 \mu\text{m}$ of air.